Dissecting the mechanisms underlying indirect genetic effects on biomedical phenotypes: a study of 170 behavioural, physiological and morphological phenotypes measured in adult laboratory mice.

Short title:

Mechanisms underlying indirect genetic effects on biomedical phenotypes

Amelie Baud[1*], Francesco Paolo Casale[1,2], Jerome Nicod[3], Oliver Stegle[1,4*]

[1] European Molecular Biology Laboratory, European Bioinformatics Institute, Wellcome Genome Campus, CB10 1SD Hinxton, Cambridge, UK

[2] Microsoft Research New England, Cambridge, Massachusetts, USA

[3] Wellcome Trust Centre for Human Genetics, Roosevelt Drive, Oxford OX3 7BN, UK

[4] European Molecular Biology Laboratory, Genome Biology Unit, Heidelberg, DE

* Corresponding authors: abaud@ebi.ac.uk and oliver.stegle@embl.de

Abstract

The phenotype of an individual can be affected not only by the individual's own genotypes (direct genetic effects, DGE) but also by genotypes of other, interacting individuals (indirect genetic effects, IGE). IGE have been detected, using polygenic models, for a broad range of biomedical phenotypes. However, little is known about the loci, genes and traits of interacting partners mediating the effects, especially where non-familial IGE are concerned. To address this question, we studied IGE arising in cages of unrelated, adult laboratory mice. We leveraged a dataset of 170 behavioural, physiological and morphological phenotypes measured in 1,812 genetically heterogeneous mice and developed two approaches. First, we used variance components models to estimate, for each phenotype, the correlation between DGE and IGE. Our results demonstrate some overlap but also differences between the mechanisms of DGE and IGE for a given phenotype. Second, we developed and applied methods for the genome-wide association study of IGE (igeGWAS) in order to identify loci, genes and traits of cage mates mediating IGE. We identified 24 genome-wide significant IGE loci for 17 phenotypes (FDR < 10%), none of which overlapped with genome-wide significant DGE loci for the same phenotype. Using an exhaustive list of single nucleotide polymorphisms at each locus, we fine-mapped each association. At six loci this pointed to a single candidate gene, which we used to formulate specific hypotheses as to the mechanisms of IGE. The empirical insights from our study and the analytical strategies we have developed pave the way for using igeGWAS to unravel mechanisms of phenotypic variation that are expressed only in the context of social interactions.

Introduction

The phenotype of an individual can be affected not only by the individual's own genotypes (direct genetic effects, DGE) but also by genotypes of other, interacting individuals (indirect genetic effects, IGE)(1-3). IGE arise when the phenotype of the "focal" individual is influenced by heritable traits of "partners", which may include behavioural and non-behavioural traits as well as modifications of the non-social environment by partners (4) (**Figure 1a**). IGE have been detected in many experimental systems(5-15), livestock(16-18), crops(19), wild animals(20-22), and humans(23-25), demonstrating that they are an important component of the genotype to phenotype path.

Most studies of IGE have used polygenic models to study aggregate effects: trait-based models(2, 26) and polygenic risk scores(24, 27) have been used to study IGE mediated by *specific* traits of partners, whereas variance components models have been used to detect IGE mediated by *any* heritable trait of partners (10, 16, 28, 29). More recently, the genome-wide association study of IGE (igeGWAS) has been proposed as a strategy to identify individual genetic loci causing IGE associations(5, 8, 9, 25, 30, 31). The major advantage of this strategy is the ability to leverage associated loci to uncover novel traits of partners influencing a phenotype of interest.

However, so far igeGWAS has been applied only in limited settings. In particular, it has not been used to study non-familial IGE affecting biomedical phenotypes (IGE from "peers"), despite evidence from polygenic models suggesting such IGE are common in laboratory mice(10) and occur in humans too(27).

In that context, it is unknown whether igeGWAS of a phenotype will identify loci other than those identified by dgeGWAS of the same phenotype. This will depend,

70 first, on the correlation between DGE and IGE for that phenotype (**Figure 1b**). This
71 correlation is expected to be different from zero based on reports of "phenotypic
72 contagion" between mouse and human peers, namely instances where an
73 intermediate phenotype such as stress levels(32-34), infection status, or a component
74 of the gut microbiome(35) is "transferred" to peers and contributes to the phenotype
75 of interest both in focal individuals and their peers. In the extreme, if the correlation
76 between DGE and IGE is close to ±1, there will be little scope for igeGWAS to identify
77 loci not identified by dgeGWAS. Second, whether igeGWAS identifies loci not
78 identified by dgeGWAS will depend on the relative power of igeGWAS and dgeGWAS,
79 which has not been thoroughly investigated.

80 Finally, when igeGWAS is applied to peer effects, each individual in the study
81 gives rise to DGE and IGE (**Figure 1b**), hence serves as both focal individual and peer
82 in the analysis. Whether this leads to confounding between DGE and IGE is unclear.

83 To address these questions, we leveraged a published dataset of 170
84 behavioural, physiological and morphological phenotypes measured in 1,812
85 genetically heterogeneous laboratory mice (**Figure 1c**), which we supplemented with
86 previously unreported cage information (**Supplementary Table 1**), and used two
87 approaches: first, we used polygenic models to estimate, for each phenotype, the
88 correlation between DGE and IGE (**blue arrows in Figure 1b**; see Methods). This
89 correlation is equivalent to the correlation between DGE on the traits of cage mates
90 influencing the phenotype of interest and DGE on the phenotype of interest itself (**red
91 arrows in Figure 1b**) and can be estimated even when the traits of cage mates
92 mediating IGE are unknown or unmeasured. Second, we developed methods for
93 igeGWAS and applied igeGWAS and dgeGWAS to the 170 phenotypes to compare

94 the relative power of dgeGWAS and igeGWAS and identify novel genes and traits of

95 cage mates mediating IGE.

96

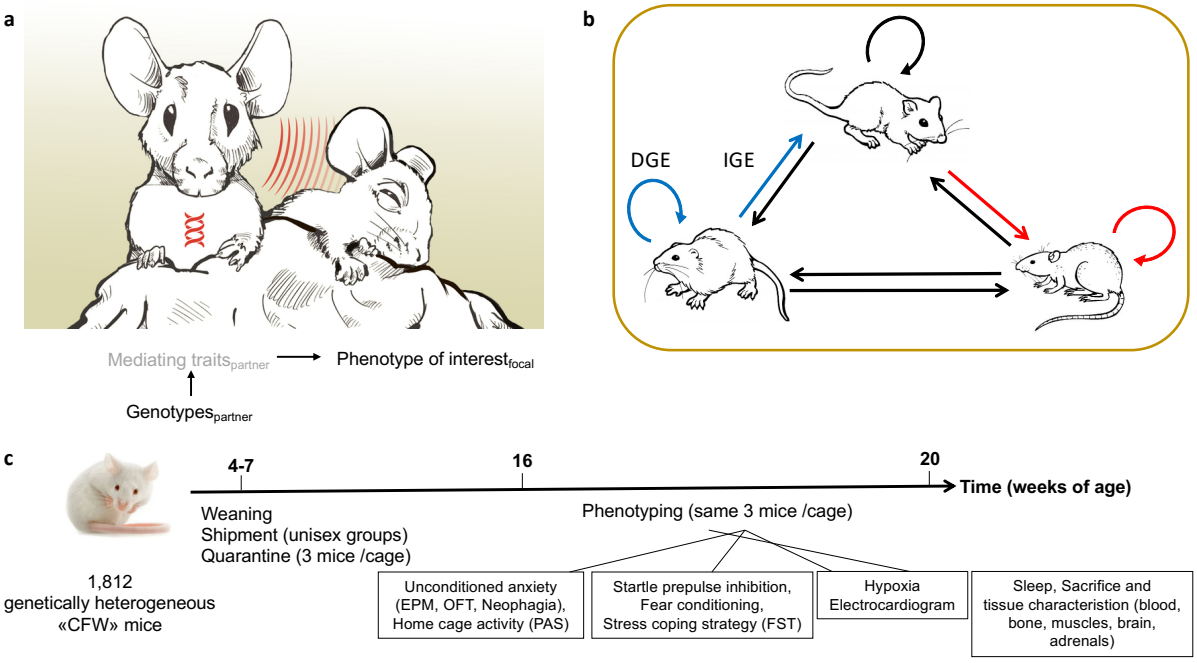

97

98 ***Figure 1*** *Illustration of indirect genetic effects (IGE) and experimental design.* ***(a)*** *IGE*

99 *arise when two individuals interact and heritable traits of one influence the phenotype*

100 *of the other. Importantly, the traits of cage mates that mediate social effects do not*

101 *need to be known or measured for many SGE analyses. This figure defines several*

102 *terms used throughout this manuscript. We further refer to "peers" as non-familial*

103 *"partners". (b) DGE and IGE when all study individuals are genetically heterogeneous.*

104 *The correlation ρ between DGE and IGE for a given phenotype is most directly*

105 *understood by looking at the blue arrows (mice "projecting" IGE). It is, however,*

106 *equivalent to the correlation between DGE on phenotype of interest and DGE on traits*

107 *of partners mediating IGE (red arrows). (c) Experimental design. A list of the 170*

108 *phenotypes collected on each mouse is presented in Supplementary Table 2.*

109

Results

We used the genome-wide genotypes (both LD-pruned and non-pruned, see Methods) and 200 phenotypes for 2,073 CFW mice reported in Nicod et al.(36) and Davies et al.(37). In addition, we used previously unreported cage information provided by the authors of the original study upon request (**Supplementary Table 1**). Mice were housed in same-sex groups and interacted for at least nine weeks before phenotyping started. For our analyses we only kept mice that had the same two cage mates over the course of the experiment. We also excluded a subset of mice suspected to be siblings in order to mitigate confounding from parental and litter effects, yielding a final sample size of 1,812 mice. We normalised each phenotype and excluded 30 phenotypes that could not be satisfactorily normalised, yielding a total of 170 phenotypes. Due to missing phenotype data, the average sample size for each phenotype was 1,256.

Correlation between DGE and IGE for a given phenotype

Initially, to assess the role of phenotypic contagion in mediating IGE and quantify the scope for igeGWAS to identify loci not identified by dgeGWAS, we used polygenic models to estimate the correlation ρ between DGE and IGE (**blue arrows in Figure 1b**). We limited our analysis to 28 traits with marginal DGE and IGE that exceeded 5%, for which ρ can be accurately estimated (**Supplementary Figure 1**), including behavioural, physiological and morphological phenotypes (**Figure 2 and Supplementary Table 2**). A correlation coefficient of 0 for a phenotype would indicate different intermediate traits (gene expression traits, pathways) mediate DGE and IGE on the phenotype of interest and no role of phenotypic contagion in mediating IGE. In

contrast, a correlation coefficient of ±1 would indicate that DGE and IGE are mediated by the exact same intermediate traits, implying that IGE are mediated by the phenotype of interest itself and that no other trait of cage mates is involved. We tested both models, finding, first, that ρ was significantly different from zero for 10 out of 28 phenotypes ($P < 0.05$), which is consistent with a role for phenotypic contagion in mediating IGE. Second, ρ was significantly different from plus or minus one for the same number of phenotypes ($P < 0.05$), indicating that phenotypic contagion is usually not sufficient to explain IGE and that traits of cage mates other than the phenotype of interest mediate IGE. To uncover those traits, we turned to igeGWAS.

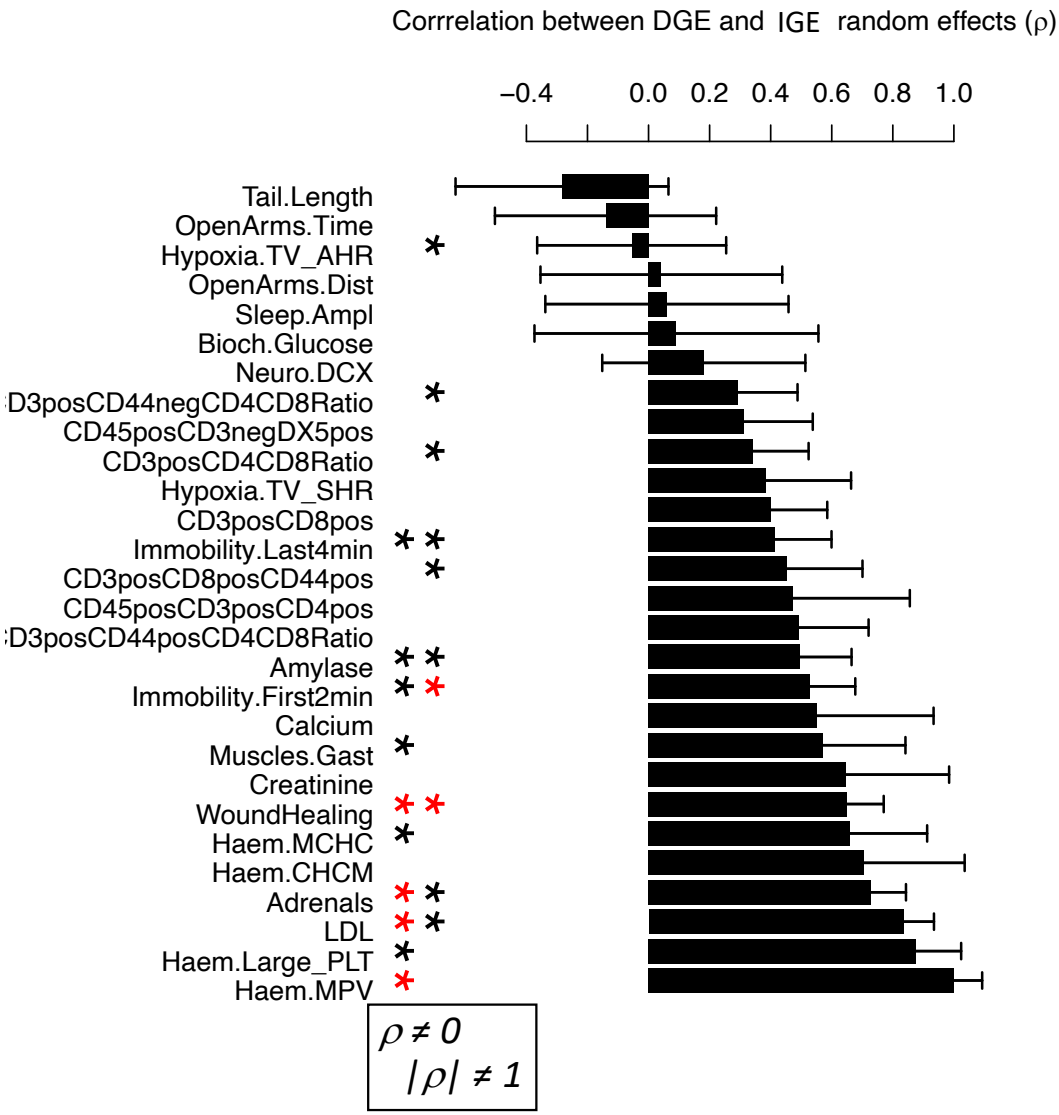

Figure 2 *Correlation coefficients ρ between DGE and IGE. ρ is shown for 28 phenotypes with marginal DGE and IGE greater than 5%. Error bars denote standard errors. Asterisks on the left show phenotypes for which ρ is significantly different from 0 (black: $P < 0.05$, red: Bonferroni-corrected $P < 0.05$). Asterisks on the right show phenotypes for which $|\rho|$ is significantly different from 1 (black: $P < 0.05$, red: Bonferroni-corrected $P < 0.05$). Numerical values are provided in Supplementary Table 2.*

154 **igeGWAS and dgeGWAS of 170 phenotypes**

155 To assess the relative power of igeGWAS and dgeGWAS and to gain insights into the
156 mechanisms of IGE, we performed igeGWAS and dgeGWAS in an analogous manner
157 for each one of the 170 phenotypes.

158 For igeGWAS, we estimated the "social genotype" of a mouse at a variant as
159 the sum of the reference allele dosages across its cage mates at the variant(31, 38),
160 and tested for association between this social genotype and the phenotype of interest.
161 In order to avoid spurious associations, we accounted for background IGE,
162 background DGE and shared environmental (cage) effects using random effect
163 components in a linear mixed model. Using simulation studies, we identified a
164 previously unrecognised source of spurious associations in igeGWAS: correlations
165 between direct and social genotypes that arise when each individual serves as both
166 focal individual and social partner in the analysis, a strategy that maximises sample
167 size when all the individuals are genotyped and phenotyped(31, 38). Importantly, we
168 show that these genotypic correlations arise even when all individuals are strictly
169 unrelated (**Supplementary Note**). To account for these correlations in our study, we
170 included, in the null model for igeGWAS, a fixed effect covariate for direct genotypes,
171 a strategy we hereafter refer to as "conditioning". Consistent with the results of a
172 simulation study, we observed that conditioning is required to obtain calibrated P
173 values (**Supplementary Figure 2, 4 and 5b**). We also note that conditioning will result
174 in decreased power to detect IGE in the absence of co-localised DGE
175 (**Supplementary Figure 3a and 3c**) but increased power if the locus also gives rise
176 to DGE (**Supplementary Figures 3b and 3d**). Given the intermediate values
177 observed for the correlation ρ between DGE and IGE across phenotypes (**Figure 2**),
178 we expect conditioning to overall increase power to detect IGE in our dataset. Finally,

179 following the approach considered in Nicod et al.(36), we employed a genome-wide
180 permutation strategy to control the FDR for each phenotype, thereby taking into
181 account the specific patterns of linkage disequilibrium present in the sample.
182 igeGWAS identified a total of 24 genome-wide significant loci across 17 of the 170
183 tested phenotypes (FDR < 10%; **Supplementary Table 3**).

184 To enable a direct comparison between igeGWAS and dgeGWAS, we ran
185 dgeGWAS for each phenotype analogously to the approach taken for igeGWAS,
186 including random effects for DGE and IGE polygenic effects and cage effects and
187 conditioning on the social genotype at each locus. This identified 120 genome-wide
188 significant DGE loci for 63 phenotypes (10% per-phenotype FDR; **Supplementary**
189 **Table 4**).

190

191 **Relative power of igeGWAS and dgeGWAS**

192 igeGWAS and dgeGWAS were run in analogous manners yet, across all 170
193 phenotypes, igeGWAS identified fewer genome-wide significant loci than dgeGWAS
194 (24 and 63 loci respectively). Consistent with this observation, genome-wide
195 significant IGE loci tended to have lower effect sizes (proportion of phenotypic
196 variance explained) than DGE loci (**Figure 3a**). This trend is likely to be even stronger
197 across all associated loci due to the Beavis effect(39, 40).

198 Was lower power to detect IGE to be expected? This question has been
199 addressed in the context of polygenic effects(41, 42) but not in the context of GWAS.
200 To do so, we carried out a power analysis where allelic effects were fixed, three
201 categories of minor allele frequencies (MAF) were considered (low, medium, or high),
202 and local DGE or IGE were simulated. We used two generative models for IGE: an
203 additive model, whereby IGE received by a focal mouse correspond to the sum of the

genetic effects projected by its cage mates, and an average model, whereby IGE received by one mouse correspond to the average of the genetic effects projected by its cage mates (see **Figure 1b**). The average model corresponds to a scenario where a mouse can only interact with one cage mate at a time, resulting in a dilution of social effects when more than one cage mate is present in the cage (two cage mates were present in this study). Our results show that power to detect IGE loci always increases with MAF and is higher than power to detect DGE if IGE arise from the sum of genetic effects across cage mates (additive model)(**Figure 3b**). With dilution however (average model), power to detect IGE becomes lower than power to detect DGE.

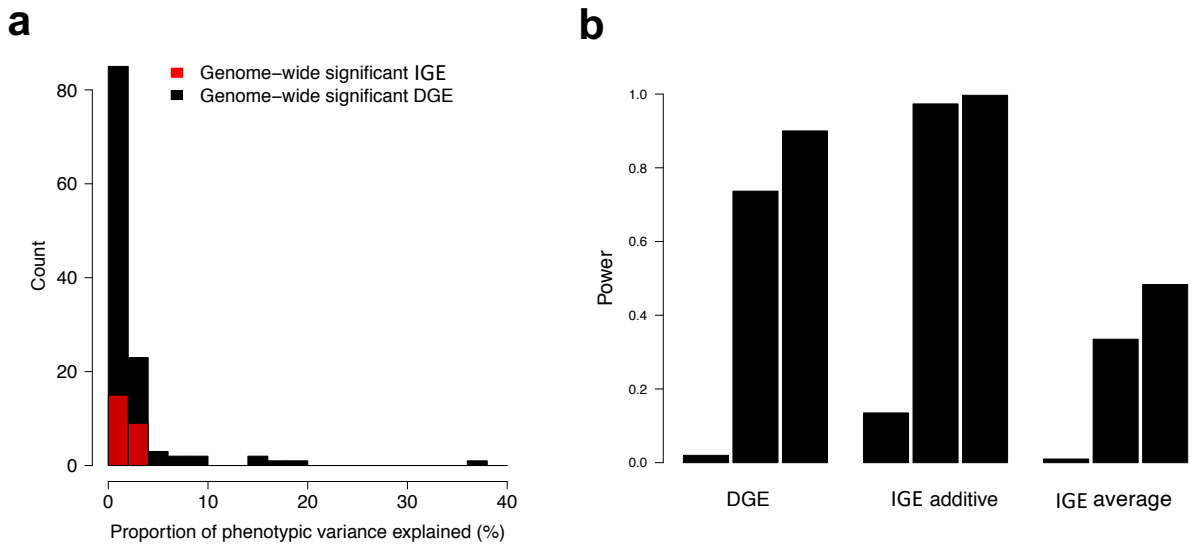

Figure 3 *Effect sizes of genome-wide significant DGE and IGE associations and relationship to power of igeGWAS and dgeGWAS.* ***(a)*** *Histogram of the proportion of phenotypic variance explained by genome-wide significant IGE (red) and DGE (black) associations (FDR < 10%).* ***(b)*** *Power to detect IGE and DGE associations in simulations. Three types of local genetic effects were simulated: DGE, IGE arising from the sum of genetic effects across cage mates (additive model) and IGE arising from the average of genetic effects across cage mates (average model). See main*

text for an explanation of the biology behind each model. For each type of effect, results are shown (left to right) for variants with low MAF (MAF < 0.05), medium MAF (0.225<MAF<0.275) and high MAF (MAF>0.45) (MAF: minor allele frequency, defined based on direct genotypes). Power was calculated at a genome-wide significance threshold of negative log P 5.

Given the relatively lower power of igeGWAS, reducing the multiple testing burden of igeGWAS by testing, for a given phenotype, only those loci that are genome-wide significant DGE loci for the same or related phenotype (e.g. DGE loci for any behavioural phenotype, or any immunological phenotype) may seem like a promising approach(12). However, we show that doing so would miss the most significant IGE loci as genome-wide significant DGE and IGE loci for a given category of phenotypes (e.g. behavioural or immunological) do not overlap (**Figure 4**). This observation is expected based on the intermediate values observed for the correlation ρ between DGE and IGE and the limited power of dgeGWAS and igeGWAS.

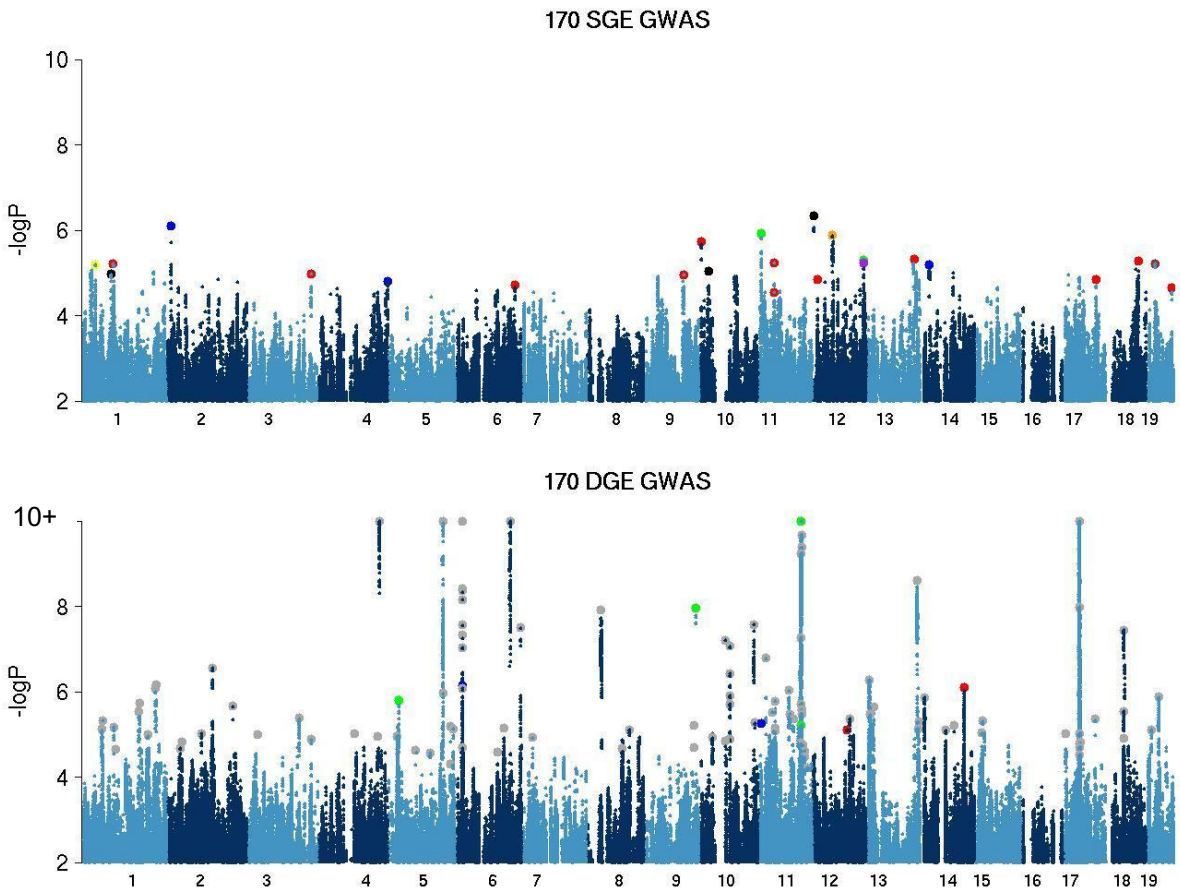

Figure 4 *Superimposed manhattan plots corresponding to igeGWAS (top panel) and dgeGWAS (bottom panel) of the same 170 phenotypes. DGE associations with a negative log P value greater than 10 were truncated at this threshold (as indicated by 10+); also, data points with negative log P values smaller than 2 are not shown. The larger dots correspond to the most significant variant at each genome-wide significant IGE or DGE locus. In the IGE panel (top), each colour corresponds to a class of phenotypes: behavioural (red, includes 7 behavioural phenotypes with a detected IGE locus), adult neurogenesis (black, 2 phenotypes), immune (orange, 1 phenotype), haematological (yellow, 1 phenotype), blood biochemistry (blue, 2 phenotypes), bone phenotypes (green, 2 phenotypes), heart function (brown, 1 phenotype), and lung function (purple, 1 phenotype). In the DGE panel (bottom), the same colouring scheme*

249 *is used as in the IGE panel except for grey dots, which are for phenotype that do not*
250 *have a genome-wide significant IGE locus.*
251
252 **Mechanisms of IGE inferred from genome-wide significant IGE loci**
253 Linkage disequilibrium decays faster in the CFW population than in many other mouse
254 populations used for mapping, which facilitates identification of putatively causal
255 genes at associated loci(36, 43, 44). To identify such genes, we fine-mapped genome-
256 wide significant IGE loci using the full set of variants (rather than the pruned set used
257 for igeGWAS) in the 1.5Mb window surrounding the most significant variant at the
258 locus, which corresponds, in this sample, to the 95% confidence interval for the
259 association(36). We then identified, for each genome-wide significant IGE locus,
260 putatively causal genes (hereafter "candidate genes") that either overlapped the
261 associated plateau or were located in direct proximity (**Supplementary Table 3**).
262 Following Nicod et al.(36), we focused on IGE loci with a single candidate gene to
263 draw hypotheses on the mechanisms of IGE.
264 *Epha4* was the only candidate gene at a locus on chromosome 1 for immobility
265 in the forced swim test (FST), a measure of stress coping strategy (**Figure 5a**, top
266 panel, and **Supplementary Figure 4**). Because direct effects of *Epha4* on FST
267 immobility have been reported(45, 46), we evaluated the possibility that behavioural
268 contagion in the weeks prior to or during the FST might mediate IGE of *Epha4* on FST
269 immobility in CFW mice. To do so, we ran a direct association (DGE) analysis using
270 the full set of variants in the same 1.5Mb window including *Epha4* as for IGE analysis.
271 We found no evidence that *Epha4* directly affects FST immobility in CFW mice (**Figure**
272 **5a**, bottom panel), making it unlikely that behavioural contagion explains the detected
273 IGE.

274 To elucidate the mechanisms of action of *Epha4*, we used independent
275 expression data from the hippocampus of a separate sample of 79 mice from the same
276 CFW population(44). We did not find a cis-eQTL for *Epha4* but identified *Dlgap1*, a
277 candidate gene at another IGE locus for FST immobility (**Supplementary Figure 5**),
278 as the sixth gene most significantly co-expressed with *Epha4* in the hippocampus of
279 CFW mice (**Supplementary Figure 6**). The correlation in expression was significant
280 after accounting for the number of genes expressed in the hippocampus (Spearman r
281 = 0.868, Bonferroni-corrected P = $2{,}3.10^{-19}$). *Epha4* and *Dlgap1* encode two synaptic
282 proteins that are important for synaptic plasticity in the hippocampus(47-49) and the
283 corresponding knock-out mice show altered social approach(50) and social
284 memory(51). Hence, our results suggest that differences in the social behaviour of
285 cage mates is responsible for IGE on stress-coping strategy in CFW mice.
286 Unfortunately, we were not able to replicate our analyses or directly test our hypothesis
287 as FST measurements were not available for the additional sample of 79 CFW mice,
288 expression data were not available for the main sample, and social behaviour was not
289 tested in either sample.

290 Among the other genome-wide significant IGE loci with a single candidate gene
291 was a locus on chromosome 12 for a measure reflecting unstable sleep patterns over
292 the three days of the sleep test (**Figure 5c**, top panel). Importantly, the mice were
293 singly housed during the sleep test, implying that any influence of cage mates must
294 have either persisted or revealed itself in the new environment that the mice
295 encountered. We found no evidence of DGE on the same measure at this locus
296 (**Figure 5c**, bottom panel), suggesting unstable sleep patterns during the sleep test
297 were not caused by similarly unstable sleep patterns of cage mates prior to the sleep
298 test.

299 The sole candidate gene at this locus, *Pgk1-rs7*, is a pseudogene of *Pgk1*,
300 which encodes the glycolytic enzyme phosphoglycerate kinase 1. Because *Pgk1* and
301 *Pgk1-rs7* have similar sequences and that could have led to genotyping errors in the
302 form of similar genotypes at *Pgk1 and Pgk1-rs7*, we first confirmed that variants in the
303 vicinity of *Pgk1-rs7* and variants in the vicinity of *Pgk1* were not linked, suggestsing
304 *Pgk1-rs7,* but not *Pgk1*, is involved. Whether *Pgk1-rs7* is functional or not has not
305 been reported before. However, the perfect sequence match between the proteins
306 encoded by *Pgk1-rs7* and *Pgk1,* evolutionary theory related to the position of *Pgk1* on
307 the X chromosome(52), and the existence of a functional pseudogene for another
308 glycolytic enzyme(53) suggest that *Pgk1-rs7* is likely to be functional.
309 A previous report found that *Pgk1-rs7* was expressed specifically in brown
310 adipose tissue - the tissue responsible for non-shivering thermogenesis – and that its
311 expression was activated by cold temperatures(54). Therefore, our hypothesis is that,
312 when mice were group-housed and slept huddled before the sleep test, heat produced
313 by cage mates raised the skin temperature of focal mice(55), which is permissive for
314 sleep(56-58); when mice became singly housed for the sleep test and as laboratory
315 conditions are well below thermoneutrality for mice(59), focal mice that used to have
316 warmer cage mates struggled more than others to adapt to the new, cold conditions,
317 resulting in unstable sleep patterns during the sleep test.
318

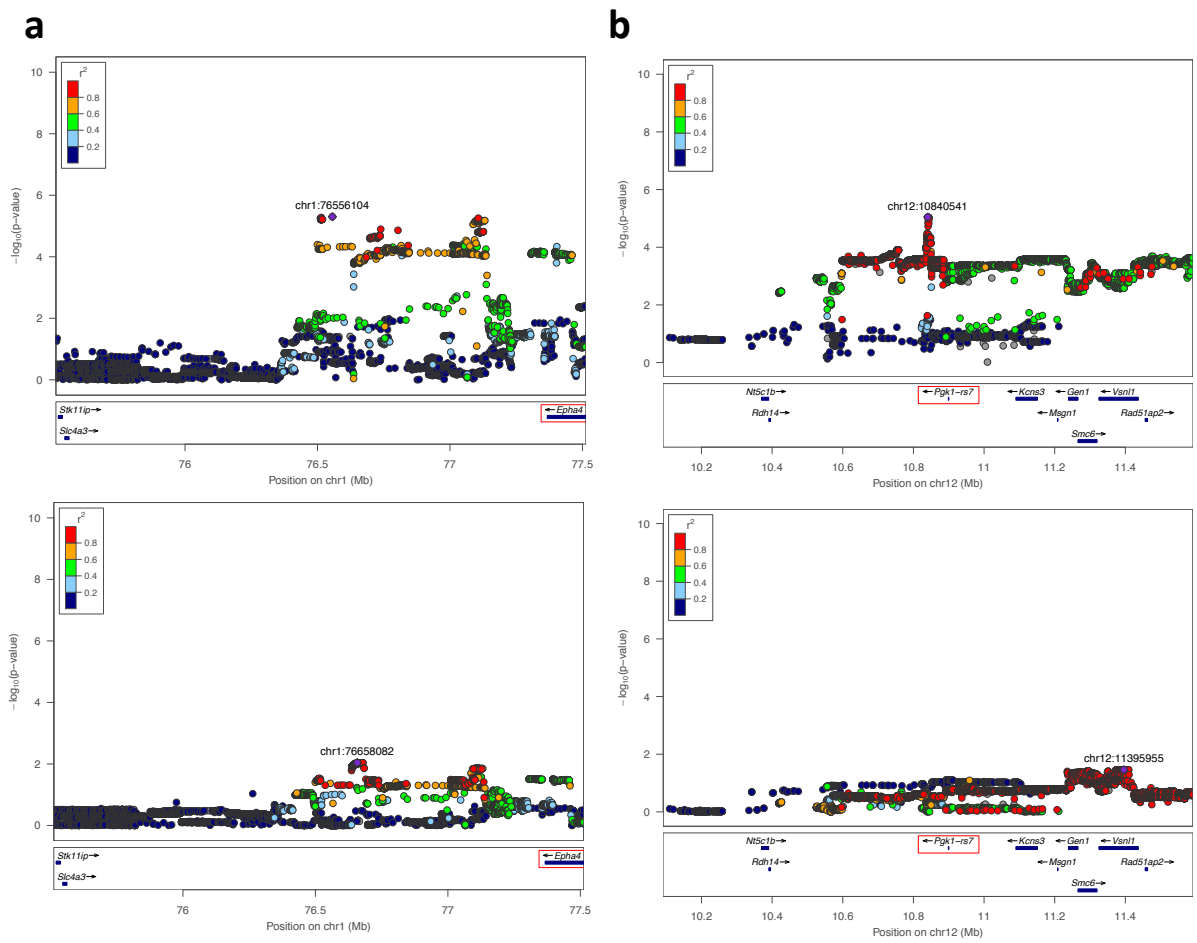

Figure 5 *Locus zoom plots for two genome-wide significant IGE loci (FDR < 10%). The top and bottom panels show, respectively, IGE and DGE associations for all the variants at the locus (rather that the set of pruned variants used for GWAS). (a) Locus on chromosome 1 for immobility during the first two minutes of the forced swim test (FST), a measure of stress-coping strategy in mice. Epha4 is the only candidate gene (see Methods) for IGE at this locus. (b) Locus on chromosome 12 for a measure reflecting unstable sleep patterns during the three days of the sleep test. Pgk1-rs7 is the only candidate gene for IGE at this locus.*

329 ## Discussion

330

331 To dissect the mechanisms underlying non-familial IGE on behavioural, physiological
332 and morphological phenotypes of adult laboratory mice(10), we applied polygenic
333 models and igeGWAS to 170 such phenotypes.

334 Using polygenic models, first, we gained insights into the role of phenotypic
335 contagion in mediating IGE and the scope for igeGWAS to identify loci not already
336 identified by dgeGWAS. To do so, we estimated, for each phenotype, the correlation
337 ρ between DGE and IGE, which is equivalent to the correlation between DGE on the
338 phenotype of interest and DGE on the (unknown, unmeasured) traits of cage mates
339 influencing the phenotype of interest. We tested two extreme scenarios: one in which
340 phenotypic contagion plays no role in mediating IGE ($\rho=0$) and one in which
341 phenotypic contagion is sufficient to explain IGE ($\rho=1$). Focusing on 28 phenotypes
342 strongly affected by DGE and IGE, we first found that ρ was significantly different from
343 0 for 10 out of 28 phenotypes ($P < 0.05$). This result is consistent with a role for
344 phenotypic contagion in mediating IGE, which is expected from previous reports of
345 phenotypic contagion following non-genetic manipulations of the phenotype of
346 laboratory mice(32, 35). We also found that ρ was significantly different from $|1|$ for 10
347 out of 28 phenotypes ($P < 0.05$), which demonstrates that phenotypic contagion is not
348 sufficient to account for IGE and that traits of cage mates other than the phenotype of
349 interest are involved.

350 Using igeGWAS, second, we identified 24 genome-wide significant IGE loci for
351 17 of the 170 phenotypes considered, none of which were genome-wide significant in
352 the corresponding dgeGWAS. We highlighted three of those loci to illustrate how IGE
353 loci may shed light into the mechanisms of IGE. Briefly, we fine-mapped each locus,

354 identified candidate genes based on their proximity to the most significantly associated
355 variants and focused, to begin with, on loci with a single candidate gene. We reviewed
356 the literature on each single candidate gene to identify traits of cage mates the gene
357 might contribute to and that could plausibly influence the phenotype of focal mice.
358 Doing so, we hypothesized a role for *Epha4* and *Dlgap1* in giving rise to IGE on
359 immobility in the FST, a measure of stress-coping strategy(60). The selective
360 improvements in social memory observed in *Epha4* knock-out mice(50) and the
361 selective reduction in social approach observed in *Dlgap1* knock-out mice(51) together
362 led us to hypothesize that variation in the social behaviour of cage mates mediates
363 IGE of *Epha4* and *Dlgap1* on stress-coping strategy. Exactly what kind of social
364 behaviour of cage mates is involved cannot be predicted from the knock-out mice, as
365 those mice were confronted to an immobilized, stranger mouse outside their home
366 cage. Similarly, evidence that both aggression from a stranger mouse and social
367 isolation affect FST immobility(61-65) supports our hypothesis but it does not
368 necessarily mean aggression or affiliative behaviour cause IGE in CFW mice.
369 Experimental work will permit testing the hypothesis that *Epha4* and *Dlgap1* can give
370 rise to IGE on stress coping strategy and identify the specific social behaviour(s)
371 involved. As a second example we highlighted an IGE locus for unstable sleep
372 patterns where *Pgk1-rs7* was the single candidate gene. Based on evidence
373 suggesting *Pgk1-rs7* is involved in non-shivering thermogenesis(54), we proposed
374 that thermogenesis in cage mates influences the sleep of focal mice by keeping the
375 skin of the latter warm as all mice sleep huddled.

376 Understanding the mechanisms underlying IGE on biomedical phenotypes in
377 laboratory mice serves two goals: first, it may uncover mechanisms of social influence
378 that are at play in humans too. For example, identifying specific aspects of the social

379 behaviour of cage mates that influence stress-coping strategy in CFW mice may
380 provide insights into specific traits of peers influencing stress-coping strategies in
381 humans. Second, improving our understanding of how mice in a cage influence each
382 other will permit measuring and accounting for relevant traits of cage mates (e.g. body
383 temperature or thermogenesis, for studies of sleep) when parameters such as DGE
384 or a drug treatment are of primary interest. In turn, this will increase the robustness
385 of mouse studies and improve translation to humans.

386 Finally, we described specific challenges for igeGWAS and proposed solutions.
387 First, using simulations we demonstrated that spurious IGE associations can arise in
388 the presence of co-localized DGE even when all mice are strictly unrelated, as a result
389 of using each mouse as a focal individual and a cage mate in the analysis. We showed
390 that conditioning on direct genotypes at the tested locus yields calibrated igeGWAS P
391 values and avoids spurious IGE associations. Second, by comparing the number of
392 genome-wide significant loci from the igeGWAS and dgeGWAS of the same 170
393 phenotypes, we showed that power is typically lower for igeGWAS compared to
394 dgeGWAS. We demonstrated that dilution of IGE across cage mates, which occurs,
395 for example, when a focal mouse can interact only with one cage mate at a time, can
396 contribute to lower power of igeGWAS.

397 The methods we have developed to estimate the correlation ρ between DGE
398 and IGE and to carry out igeGWAS are very general and appropriate for many different
399 types of experimental designs. Together with the insights gained from our analysis of
400 170 phenotypes, they pave the way for future igeGWAS of biomedical phenotypes in
401 laboratory mice.

402

403 # Materials and methods

404

405 **Phenotypes and experimental variables**

406 Phenotypes and experimental variables (covariates) for 1,934 Crl:CFW(SW)-US_P08
407 (CFW) mice were retrieved from http://wp.cs.ucl.ac.uk/outbredmice/. Phenotypes
408 were normalized using the boxcox function (MASS package[64]) in R; phenotypes that
409 could not be normalised satisfactorily (transformation parameter lambda outside of -2
410 to 2 interval) were excluded. The subset of covariates used for each phenotype is
411 indicated in Supplementary Table 2. Because data for some phenotypes were missing
412 for some mice, the sample size varied. The sample size for each phenotype after all
413 filtering (see below) is indicated in Supplementary Table 2.

414

415 **Cage information**

416 Mice were four to seven weeks old when they arrived at the phenotyping facility and
417 were housed in same-sex groups of three mice. They were left undisturbed for nine to
418 twelve weeks during their time in quarantine and spent another four weeks together
419 during phenotyping.

420 Cage assignments were not included in the publicly available dataset but were
421 provided by the authors upon request and are now provided in **Supplementary Table**
422 **1**. Cage assignments were recorded at eleven time points throughout the study and
423 showed that a few mice were taken out of their original cages and singly housed,
424 presumably because they were too aggressive. We only included in our analyses mice
425 that had the same two cage mates throughout the experiment. We further excluded a
426 subset of mice based on their genotype-based genetic similarity, as described below.

427 Finally, all mice were singly housed during the sleep test and until sacrifice a few days
428 later. Hence, we investigated "persistent" IGE on sleep and tissue phenotypes.
429
430 **Genome-wide genotypes**
431 From http://wp.cs.ucl.ac.uk/outbredmice/ we retrieved both allele dosages for 7 million
432 variants and allele dosages for a subset of 353,697 high quality, LD-pruned variants
433 (as described in Nicod et al.[38]; genotyping based on sparse sequencing data). We
434 used high quality, LD-pruned variants for all analyses but the identification of candidate
435 genes at IGE loci (see below), for which we used the full set of variants.
436
437 **Genetic relatedness matrix (GRM) and exclusion of presumed siblings**
438 The genetic relatedness matrix was calculated as the cross-product of the LD-pruned
439 dosage matrix after standardizing the dosages for each variant to mean 0 and variance
440 1. A few pairs of mice were outliers in the distribution of GRM values, which made us
441 suspect that siblings had been included in the sample even though they were not
442 supposed to be (siblings were excluded by design). To mitigate confounding of DGE
443 and IGE analyses by litter effects, we excluded 19 cages (57 mice) from all analyses.
444
445 **Variance components model**
446 The same model as described in detail in Baud et al.[11] was used. Briefly, the model
447 used is the following:
448 $$y_f = X_f \underline{b} + a_{D,f} + e_{D,f} + Z_f \underline{a_S} + Z_f \underline{e_S} + W_f \underline{c} \qquad (0)$$
449 y_f is the phenotypic value of the focal mouse f, X_f is a row of the matrix X of covariate
450 values and b a column vector of corresponding estimated coefficients. $\underline{a_{D,f}}$ is the
451 additive direct genetic effects (DGE) of f. Z_f is a row of the matrix Z that indicates

cage mates (importantly $Z_{i,i} = 0$) and $\underline{a_S}$ the column vector of additive indirect (social) genetic effects (IGE). $\underline{e_D}$ refers to direct environmental effects (DEE) and $\underline{e_S}$ to indirect (social) environmental effects (IEE). W_f is a row of the matrix W that indicates cage assignment and c the column vector of cage effects.

The joint distribution of all random effects is defined as:

$$\begin{bmatrix} \underline{a_D} \\ \underline{a_S} \\ \underline{e_D} \\ \underline{e_S} \\ \underline{c} \end{bmatrix} \sim \mathrm{MVN}\left(0, \begin{bmatrix} \sigma^2_{A_D}\mathrm{A} & \sigma_{A_{DS}}\mathrm{A} & 0 & 0 & 0 \\ \sigma_{A_{DS}}\mathrm{A}^T & \sigma^2_{A_S}\mathrm{A} & 0 & 0 & 0 \\ 0 & 0 & \sigma^2_{E_D}\mathrm{I} & \sigma_{E_{DS}}\mathrm{I} & 0 \\ 0 & 0 & \sigma_{E_{DS}}\mathrm{I}^T & \sigma^2_{E_S}\mathrm{I} & 0 \\ 0 & 0 & 0 & 0 & \sigma^2_C\mathrm{I} \end{bmatrix}\right)$$

where A is the GRM matrix and I the identity matrix.

The phenotypic covariance is:

$$C_{i,j} = cov\left(y_i, y_j\right) = \sigma^2_{A_D} A_{i,j} + \sigma_{A_{DS}}\left\{(AZ^T)_{i,j} + (ZA^T)_{i,j}\right\} + \sigma^2_{A_S}(ZAZ^T)_{i,j}$$
$$+ \sigma^2_{E_D} I_{i,j} + \sigma_{E_{DS}}\left\{(IZ^T)_{i,j} + (ZI^T)_{i,j}\right\} + \sigma^2_{E_S}(ZIZ^T)_{i,j}$$
$$+ \sigma^2_C (WIW^T)_{i,j}$$

The variances explained by DGE and IGE were calculated respectively as

$sampleVar\left(\sigma^2_{A_D} A\right) / sampleVar(C)$ and $sampleVar\left(\sigma^2_{A_S}(ZAZ^T)\right) / sampleVar(C)$

where $sampleVar$ is the sample variance of the corresponding covariance matrix: suppose that we have a vector $\underline{x}$ of random variables with covariance matrix M, the sample variance of M is calculated as

$$sampleVar(M) = \frac{Tr(PMP)}{n-1}$$

Tr denotes the trace, n is the sample size, and $P = I - \frac{11'}{n}$ [65,66].

For those phenotypes where body weight was included as a covariate, we checked that this did not lead to systematically increased (or decreased) estimates of the aggregate contribution of IGE (collider bias).

Significance of the IGE variance component was assessed using a two-degree of freedom log likelihood ratio (LLR) test (for the variance component and the covariance with DGE). Note that this testing procedure is conservative. The Q value for the aggregate contribution of IGE was calculated for each phenotype using the R package qvalue[67]. Significant IGE contributions were reported at FDR < 10% (corresponding to Q value < 0.1).

Alternative use of a less general model

When all cages have the same number of mice, as is the case in this study, the non-genetic random effects are not identifiable[17,68]. An equivalent model can, in that case, be defined as:

$cov\left(e_i, e_j\right) = \sigma_E^2 = \sigma_{E_D}^2 + \sigma_{E_S}^2 + \sigma_C^2$ if $i = j$

$cov\left(e_i, e_j\right) = \rho\sigma_E^2 = 2\,\sigma_{E_{DS}} + \sigma_C^2$ if $i \neq j$ and i and j share a cage

$cov\left(e_i, e_j\right) = 0$ if i and j are in different cages

We checked that both model (0) and this alternative model yielded the same genetic estimates and maximum likelihoods. The alternative model was fitted using the SimplifNonIdableEnvs option in LIMIX.

Correlation between DGE and IGE

The correlation ρ between $\underline{a_D}$ and $\underline{a_S}$ was calculated as:

$$\rho = \frac{\sigma_{A_{DS}}}{\sigma_{A_D} \times \sigma_{A_S}}$$

We tested whether ρ was significantly different from 0 and whether |ρ| was significantly different from 1 using a one-degree of freedom LLR test.

497 **Simulations for Supplementary Figure 1.**

498 Phenotypes were simulated based on the genotypes and cage relationships of the full
499 set of 1,812 mice. Phenotypes were drawn from model (0) with the following
500 parameters: IGE explaining between 0 and 35.7% of phenotypic variance, DGE
501 explaining 15% of phenotypic variance, $\rho_{A_{DS}}$= 0.47, DEE explaining 22% pf phenotypic
502 variance, IEE explaining 16% of phenotypic variance, $\rho_{E_{DS}}$ = -0.97, and cage effects
503 explaining 26% of phenotypic variance. These variances correspond to the median
504 value of estimates across traits with aggregate IGE and DGE > 5%. After building the
505 phenotypic covariance matrix, the sample variance of the simulations was calculated
506 and used to calculate "realised" simulation parameters from the "target" parameters
507 above. The realised parameters were used for comparison with the parameters
508 estimated from the simulations.

509

510 **Definition of "social genotype" for igeGWAS**

511 We assumed additive effects across cage mates and calculated the "social genotype"
512 of a mouse as the sum of the reference allele dosages of its cage mates. The same
513 assumption was made by Biscarini *et al.*[37] and Brinker *et al.*[28] among others.

514

515 **Correlation between direct and social genotypes at a variant (Supplementary**
516 **Figure 2)**

517 Spearman's rank correlation coefficient was used. We tested whether the correlation
518 was different from 0 using the function cor.test in the R package stats[69].

519

520 **Models used for igeGWAS and dgeGWAS**

521 To test IGE of a particular variant, we compared the following two models:

522 $y_f = X_f\underline{b} + a_{D,f} + e_{D,f} + Z_f\underline{a_S} + Z_f\underline{e_S} + W_f\underline{c} + G_f b_D$ (1, null)

523 $y_f = X_f\underline{b} + a_{D,f} + e_{D,f} + Z_f\underline{a_S} + Z_f\underline{e_S} + W_f\underline{c} + G_f b_D + Z_f G b_S$ (2, alternative)

524 Here, G is the vector of direct genotypes at the tested variant, b_D the estimated
525 coefficient for local DGE and b_S the estimated coefficient for local IGE. In igeGWAS,
526 we refer to the inclusion of $G_f b_D$ in model (1, null) as "conditioning".

527 The models were fitted using LIMIX[70,71] with the covariance of the model
528 estimated only once per phenotype, in the null model with no local genetic effect
529 (model 0).

530 The significance of local IGE was calculated by comparing models (1) and (2)
531 with a 1-degree of freedom LLR test.

532 dgeGWAS was carried out by comparing model (2) above to the null model (3)
533 below:

534 $y_f = X_f\underline{b} + a_{D,f} + e_{D,f} + Z_f\underline{a_S} + Z_f\underline{e_S} + W_f\underline{c} + Z_f G b_S$ (3, null)

535 In dgeGWAS, we refer to the inclusion of $Z_f G b_S$ in model (3, null) as "conditioning".

536

537 **Identification of genome-wide significant associations**

538 We used a genome-wide permutation strategy to control the FDR for each phenotype,
539 as done by Nicod et al.(36). This strategy takes into account the specific patterns of
540 linkage disequilibrium present in the sample and identifies genome-wide significant
541 associations *for each phenotype independently of the results for the other phenotypes*
542 *in the dataset*. More precisely, for each phenotype and for each type of genetic effect
543 (social and direct), we performed 100 "permuted GWAS" by permuting the rows of the
544 matrix of social (respectively direct) genotypes, and testing each variant at a time using
545 the permuted genotypes together with the un-permuted phenotypes, un-permuted
546 covariates, un-permuted GRM and un-permuted matrix of direct (respectively social)

547 genotypes (for conditioning). See [71,73] for references on this permutation approach.
548 For a given P value x, the per-phenotype FDR can be calculated as:

549 $$FDR(x) = \frac{\#\ loci\ with\ P < x\ in\ permuted\ data}{100\ \times\ \#\ loci\ with\ P < x\ in\ unpermuted\ data}$$

550 We reported those loci with FDR < 10%.

551

552 **Definition of candidate genes at associated loci**

553 At each significantly associated locus we defined a 1.5Mb window centred on the lead
554 variant corresponding, in this sample, to the 95% confidence interval for the
555 association[38]. We identified all the variants that segregate in this window based on the
556 full set of 7M variants and reran igeGWAS and dgeGWAS locally using all the variants
557 at the locus. We defined "candidate" genes as those genes that either overlapped the
558 associated plateau or were located in direct proximity, and whose MGI symbol does
559 not start by 'Gm', 'Rik', 'Mir', 'Fam', or 'Tmem' in order to focus on genes with known
560 function and generate more tractable hypotheses on the pathways of social effects.

561

562 **Gene expression in the hippocampus of an independent sample of CFW mice**

563 Gene expression in the hippocampus of an independent sample of 79 male CFW mice,
564 initially published in Parker et al.[40], was available from GeneNetwork
565 (http://gn2.genenetwork.org/). The data are accessible by selecting Mouse as
566 *Species*, CFW Outbred GWAS as *Group*, Hippocampus mRNA as *Type*, and UCSD
567 CFW Hippocampus (Jan17) RNA-Seq Log2 Z-score as *Dataset*. To retrieve the genes
568 whose expression is most highly correlated with that of *Epha4*, we entered "Epha4" in
569 the *Get Any* field. Following selection of the Epha4 record (click on
570 ENSMUSG00000026235), we used *Calculate Correlations* with Sample r as *Method*,
571 UCSD CFW Hippocampus (Jan17) RNA-Seq Log2 Z-score as *Database*, and

572 Spearman rank as correlation *Type*. Supplementary Figure 6 was obtained by clicking
573 on the value of the correlation between Epha4 and Dlgap1 expression levels (column
574 *Sample rho*).
575
576 **Variance explained by a genome-wide significant association**
577 The variance explained by a genome-wide significant IGE association was estimated
578 in an extension of model (0) with additional fixed effects for both direct and social
579 effects of lead SNPs at all genome-wide significant IGE loci (the lead SNP being the
580 SNP with the most significant P value at the locus in the igeGWAS). After fitting the
581 model, the variance was calculated as:

583 $$\frac{var(ZG\widehat{b_S})}{\sum var\left(X_c\widehat{b_c}\right) + \sum var\left(G\widehat{b_D}\right) + \sum var(ZG\widehat{b_S}) + sampleVar(C)}$$

582 where $sampleVar(C)$ is the sample variance of the covariance matrix in this model.
584 The variance explained by a genome-wide significant DGE association was
585 estimated in a similar model but considering all genome-wide significant DGE
586 associations and
587 calculated as:

589 $$\frac{var(ZG\widehat{b_D})}{\sum var\left(X_c\widehat{b_c}\right) + \sum var\left(G\widehat{b_D}\right) + \sum var(ZG\widehat{b_S}) + sampleVar(C)}$$

588
590 **Simulations for Supplementary Figure 2c and 2d.**
591 Phenotypes were simulated based on the genotypes and cage relationships of the
592 1,812 mice. Phenotypes were simulated as the sum of random effects and local DGE
593 (from model (1)), with the following parameters: $\sigma^2_{A_D}$ = 5 or 20, $\sigma^2_{A_S}$ = 5 or 20, $\rho_{A_{DS}}$= 0.5,
594 $\sigma^2_{E_D}$= 30, $\sigma^2_{E_S}$= 30, $\rho_{E_{DS}}$ = -0.97, σ^2_C = 25. The values for $\rho_{A_{DS}}$, $\sigma^2_{E_D}$, $\sigma^2_{E_S}$, $\rho_{E_{DS}}$, and σ^2_C

were close to the median of the corresponding estimates from the real data. $\sigma^2_{A_D} = 5$ and $\sigma^2_{A_S} = 5$ correspond to low polygenic effects in the real data, and $\sigma^2_{A_D} = 20$ and $\sigma^2_{A_S} = 20$ correspond to high polygenic effects in the real data. We simulated local DGE at random variants in the genome, and simulated variances of 0, 5, 20 or 50.

The results we show in Supplementary Figure 2c and 2d are based on a subset of simulations: $\sigma^2_{A_D} = 20$ and $\sigma^2_{A_S} = 20$ and local DGE variance of 20.

Simulations for Supplementary Figure 3a-d, and Figure 3a.

Phenotypes were simulated based on the real genotypes but random cages. Phenotypes were simulated as the sum of random effects, local DGE and local IGE (model (2)) with the following parameters: $\sigma^2_{A_D}$ = 17, $\sigma^2_{A_S}$ = 17, $\rho_{A_{DS}}$= 0.65, $\sigma^2_{E_D}$= 19, $\sigma^2_{E_S}$= 15, $\rho_{E_{DS}}$ = -0.8, σ^2_C = 25. Those values correspond to the median estimates for phenotypes with aggregate IGE and DGE > 0.1.

We simulated local IGE and DGE at variants where direct and social genotypes were either lowly correlated (Spearman correlation negative log P value < 0.05) or more highly correlated (Spearman correlation negative log P value > 0.2), and had with low MAF (MAF < 0.05), medium MAF (0.225<MAF<0.275) or high MAF (MAF>0.45). We simulated local DGE with an allelic effect of 0 or 1 (1 corresponds to a large effect in the real data). We simulated local IGE under two alternative generative models: an “additive” model by using Z as in model (2) (i.e. filled with 0s and 1s) or a “proportional” model by using $Z' = \frac{Z}{N}$. In all cases we simulated an allelic effect of 0.2 (similar to the average allelic effect estimated in the IGE GWAS). The sample variance of the simulated local DGE term is $var(Gb_D) = 2p(1-p)\, b_D^2$; it is $var(ZGb_S) = 2Np(1-p)\, b_S^2$ for the local IGE term simulated under the additive model, and

619 $var\left(\frac{Z}{N}Gb_S\right) = \frac{2Np(1-p)}{N^2}b_S^2$ for the local IGE component simulated under the
620 proportional model.

621 The results we show in Supplementary Figure 3a-d are based on simulations
622 averaged across low, medium and high MAF. Power was calculated at a genome-wide
623 significance threshold of negative log P 5, which is similar to the significance of
624 associations detected at FDR < 10%.

625 The results we show in Figure 3b are based on a subset of simulations with no
626 local DGE, averaged across high and low genotypic correlations. Power was also
627 calculated at a genome-wide significance threshold of negative log P 5.

628

629 ## Scripts used in this study

630 All the scripts used in this study are available from http://github.com/limix/IGE.
631 LIMIX can be downloaded from http://github.com/limix/limix.

632

633 ## Acknowledgements

634 The authors want to thank Drs. Na Cai and Robert W. Davies and Richard Mott for
635 facilitating access to the genotype data from Nicod et al.(36), as well as Dr. Paul
636 Franken for a discussion of the sleep measure reported in this manuscript. AB was
637 supported by a fellowship from the Wellcome Trust (105941/Z/14/Z).

638

639 ## Authors' contributions

640 AB and OS designed the study. AB and FPC performed the analyses. AB, FPC, JN
641 and OS interpreted the results. AB and OS wrote the manuscript with input from FPC
642 and JN.

643 # References

644 1. Griffing B. Selection in reference to biological groups I. Individual and group selection
645 applied to populations of unordered groups. Australian Journal of Biological Sciences.
646 1967;20(1):127-40.
647 2. Moore AJ, Brodie III ED, Wolf JB. Interacting phenotypes and the evolutionary
648 process: I. Direct and indirect genetic effects of social interactions. Evolution.
649 1997;51(5):1352-62.
650 3. Wolf JB, Brodie III ED, Cheverud JM, Moore AJ, Wade MJ. Evolutionary
651 consequences of indirect genetic effects. Trends in ecology & evolution. 1998;13(2):64-9.
652 4. Wolf JB, Mutic JJ, Kover PX. Functional genetics of intraspecific ecological
653 interactions in Arabidopsis thaliana. Philosophical Transactions of the Royal Society B:
654 Biological Sciences. 2011;366(1569):1358-67.
655 5. Bailey NW, Hoskins JL. Detecting cryptic indirect genetic effects. Evolution.
656 2014;68(7):1871-82.
657 6. Beck JA, Lloyd S, Hafezparast M, Lennon-Pierce M, Eppig JT, Festing MF, et al.
658 Genealogies of mouse inbred strains. Nature genetics. 2000;24(1):23-5.
659 7. Bleakley BH, Brodie ED. Indirect genetic effects influence antipredator behavior in
660 guppies: estimates of the coefficient of interaction psi and the inheritance of reciprocity.
661 Evolution. 2009;63(7):1796-806.
662 8. Ashbrook DG, Gini B, Hager R. Genetic variation in offspring indirectly influences the
663 quality of maternal behaviour in mice. Elife. 2015;4:11814.
664 9. Ashbrook DG, Sharmin N, Hager R, editors. Offspring genes indirectly influence
665 sibling and maternal behavioural strategies over resource share. Proc R Soc B; 2017: The Royal
666 Society.

667 10. Baud A, Mulligan MK, Casale FP, Ingels JF, Bohl CJ, Callebert J, et al. Genetic
668 variation in the social environment contributes to health and disease. PLoS genetics.
669 2017;13(1):e1006498.
670 11. Head ML, Berry LK, Royle NJ, Moore AJ. Paternal care: direct and indirect genetic
671 effects of fathers on offspring performance. Evolution. 2012;66(11):3570-81.
672 12. Mutic JJ, Wolf JB. Indirect genetic effects from ecological interactions in Arabidopsis
673 thaliana. Molecular ecology. 2007;16(11):2371-81.
674 13. Petfield D, Chenoweth SF, Rundle HD, Blows MW. Genetic variance in female
675 condition predicts indirect genetic variance in male sexual display traits. Proceedings of the
676 National Academy of Sciences. 2005;102(17):6045-50.
677 14. Wilson AJ, Gelin U, Perron M-C, Réale D. Indirect genetic effects and the evolution of
678 aggression in a vertebrate system. Proceedings of the Royal Society of London B: Biological
679 Sciences. 2009;276(1656):533-41.
680 15. Moore AJ, Haynes KF, Preziosi RF, Moore PJ. The evolution of interacting
681 phenotypes: genetics and evolution of social dominance. the american naturalist.
682 2002;160(S6):S186-S97.
683 16. Bergsma R, Kanis E, Knol EF, Bijma P. The contribution of social effects to heritable
684 variation in finishing traits of domestic pigs (Sus scrofa). Genetics. 2008;178(3):1559-70.
685 17. Ellen ED, Visscher J, van Arendonk JA, Bijma P. Survival of laying hens: genetic
686 parameters for direct and associative effects in three purebred layer lines. Poultry science.
687 2008;87(2):233-9.
688 18. Alemu SW, Bijma P, Møller SH, Janss L, Berg P. Indirect genetic effects contribute
689 substantially to heritable variation in aggression-related traits in group-housed mink (Neovison
690 vison). Genetics Selection Evolution. 2014;46(1):30.

691 19. e Silva JC, Potts B, Gilmour A, Kerr R. Genetic-based interactions among tree
692 neighbors: identification of the most influential neighbors, and estimation of correlations
693 among direct and indirect genetic effects for leaf disease and growth in Eucalyptus globulus.
694 Heredity. 2017;119(3):125.
695 20. Wilson A, Coltman D, Pemberton J, Overall A, Byrne K, Kruuk L. Maternal genetic
696 effects set the potential for evolution in a free-living vertebrate population. Journal of
697 evolutionary biology. 2005;18(2):405-14.
698 21. McAdam AG, Boutin S, Réale D, Berteaux D. Maternal effects and the potential for
699 evolution in a natural population of animals. Evolution. 2002;56(4):846-51.
700 22. Hadfield JD, Burgess MD, Lord A, Phillimore AB, Clegg SM, Owens IP. Direct versus
701 indirect sexual selection: genetic basis of colour, size and recruitment in a wild bird.
702 Proceedings of the Royal Society B: Biological Sciences. 2006;273(1592):1347-53.
703 23. Bates TC, Maher BS, Medland SE, McAloney K, Wright MJ, Hansell NK, et al. The
704 Nature of Nurture: Using a Virtual-Parent Design to Test Parenting Effects on Children's
705 Educational Attainment in Genotyped Families. Twin Research and Human Genetics. 2018:1-
706 11.
707 24. Kong A, Thorleifsson G, Frigge ML, Vilhjalmsson BJ, Young AI, Thorgeirsson TE, et
708 al. The nature of nurture: Effects of parental genotypes. Science. 2018;359(6374):424-8.
709 25. Warrington NM, Beaumont RN, Horikoshi M, Day FR, Helgeland Ø, Laurin C, et al.
710 Maternal and fetal genetic effects on birth weight and their relevance to cardio-metabolic risk
711 factors. Nature genetics. 2019:1.
712 26. McGlothlin JW, Brodie III ED. HOW TO MEASURE INDIRECT GENETIC
713 EFFECTS: THE CONGRUENCE OF TRAIT-BASED AND VARIANCE-PARTITIONING
714 APPROACHES. Evolution. 2009;63(7):1785-95.

715 27. Sotoudeh R, Harris KM, Conley D. Effects of the peer metagenomic environment on
716 smoking behavior. Proceedings of the National Academy of Sciences. 2019;116(33):16302-7.
717 28. Bijma P. The quantitative genetics of indirect genetic effects: a selective review of
718 modelling issues. Heredity. 2014;112(1):61.
719 29. Wilson AJ, Morrissey M, Adams M, Walling CA, Guinness FE, Pemberton JM, et al.
720 Indirect genetics effects and evolutionary constraint: an analysis of social dominance in red
721 deer, Cervus elaphus. Journal of evolutionary biology. 2011;24(4):772-83.
722 30. McGinnis R, Steinthorsdottir V, Williams NO, Thorleifsson G, Shooter S, Hjartardottir
723 S, et al. Variants in the fetal genome near FLT1 are associated with risk of preeclampsia. Nature
724 genetics. 2017;49(8):1255.
725 31. Brinker T, Bijma P, Vereijken A, Ellen ED. The genetic architecture of socially-
726 affected traits: a GWAS for direct and indirect genetic effects on survival time in laying hens
727 showing cannibalism. Genetics Selection Evolution. 2018;50(1):38.
728 32. de Oliveira PC, Zaniboni CR, Carmona IM, Fonseca AR, Canto-de-Souza A.
729 Preliminary behavioral assessment of cagemates living with conspecifics submitted to chronic
730 restraint stress in mice. Neuroscience letters. 2017;657:204-10.
731 33. Bolger N, DeLongis A, Kessler RC, Wethington E. The contagion of stress across
732 multiple roles. Journal of Marriage and the Family. 1989:175-83.
733 34. Haeffel GJ, Hames JL. Cognitive Vulnerability to Depression Can Be Contagious.
734 Clinical Psychological Science. 2014;2(1):75-85.
735 35. Ridaura VK, Faith JJ, Rey FE, Cheng J, Duncan AE, Kau AL, et al. Gut microbiota
736 from twins discordant for obesity modulate metabolism in mice. Science.
737 2013;341(6150):1241214.

738 36. Nicod J, Davies RW, Cai N, Hassett C, Goodstadt L, Cosgrove C, et al. Genome-wide
739 association of multiple complex traits in outbred mice by ultra-low-coverage sequencing.
740 Nature genetics. 2016;48(8):912.
741 37. Davies RW, Flint J, Myers S, Mott R. Rapid genotype imputation from sequence
742 without reference panels. Nature genetics. 2016;48(8):965.
743 38. Biscarini F, Bovenhuis H, Van Der Poel J, Rodenburg T, Jungerius A, Van Arendonk
744 J. Across-line SNP association study for direct and associative effects on feather damage in
745 laying hens. Behavior genetics. 2010;40(5):715-27.
746 39. Beavis W. QTL analyses: power, precision and accuracy. Molecular Dissection of
747 Complex Traits. Edited by: AH P. 1997. CRC Press, New York.
748 40. Beavis W, Beavis W. The power and deceit of QTL experiments: lessons from
749 comparative QTL studies. 1994.
750 41. Bijma P. Estimating indirect genetic effects: precision of estimates and optimum
751 designs. Genetics. 2010;186(3):1013-28.
752 42. Bijma P. Multilevel selection 4: modeling the relationship of indirect genetic effects
753 and group size. Genetics. 2010;186(3):1029-31.
754 43. Yalcin B, Nicod J, Bhomra A, Davidson S, Cleak J, Farinelli L, et al. Commercially
755 available outbred mice for genome-wide association studies. PLoS genetics.
756 2010;6(9):e1001085.
757 44. Parker CC, Gopalakrishnan S, Carbonetto P, Gonzales NM, Leung E, Park YJ, et al.
758 Genome-wide association study of behavioral, physiological and gene expression traits in
759 outbred CFW mice. Nature genetics. 2016;48(8):919.
760 45. Li Y, Wang H, Wang X, Liu Z, Wan Q, Wang G. Differential expression of
761 hippocampal EphA4 and ephrinA3 in anhedonic-like behavior, stress resilience, and

762 antidepressant drug treatment after chronic unpredicted mild stress. Neuroscience letters.
763 2014;566:292-7.
764 46. Zhang J-c, Yao W, Qu Y, Nakamura M, Dong C, Yang C, et al. Increased EphA4-
765 ephexin1 signaling in the medial prefrontal cortex plays a role in depression-like phenotype.
766 Scientific Reports. 2017;7(1):7133.
767 47. Bouvier D, Corera AT, Tremblay MÈ, Riad M, Chagnon M, Murai KK, et al. Pre-
768 synaptic and post-synaptic localization of EphA4 and EphB2 in adult mouse forebrain. Journal
769 of neurochemistry. 2008;106(2):682-95.
770 48. Murai KK, Nguyen LN, Irie F, Yamaguchi Y, Pasquale EB. Control of hippocampal
771 dendritic spine morphology through ephrin-A3/EphA4 signaling. Nature neuroscience.
772 2003;6(2):153-60.
773 49. Coba M, Ramaker M, Ho E, Thompson S, Komiyama N, Grant S, et al. Dlgap1
774 knockout mice exhibit alterations of the postsynaptic density and selective reductions in
775 sociability. Scientific reports. 2018;8(1):1-12.
776 50. Poppe L, Rué L, Timmers M, Lenaerts A, Storm A, Callaerts-Vegh Z, et al. EphA4 loss
777 improves social memory performance and alters dendritic spine morphology without changes
778 in amyloid pathology in a mouse model of Alzheimer's disease. Alzheimer's Research &
779 Therapy. 2019;11(1):1-13.
780 51. Coba M, Ramaker M, Ho E, Thompson S, Komiyama N, Grant S, et al. Dlgap1
781 knockout mice exhibit alterations of the postsynaptic density and selective reductions in
782 sociability. Scientific reports. 2018;8(1):2281.
783 52. Marques AC, Dupanloup I, Vinckenbosch N, Reymond A, Kaessmann H. Emergence
784 of young human genes after a burst of retroposition in primates. PLoS biology.
785 2005;3(11):e357.

786 53. Betrán E, Wang W, Jin L, Long M. Evolution of the phosphoglycerate mutase
787 processed gene in human and chimpanzee revealing the origin of a new primate gene.
788 Molecular biology and evolution. 2002;19(5):654-63.
789 54. Cheng Y, Jiang L, Keipert S, Zhang S, Hauser A, Graf E, et al. Prediction of Adipose
790 Browning Capacity by Systematic Integration of Transcriptional Profiles. Cell reports.
791 2018;23(10):3112-25.
792 55. Sokoloff G, Blumberg MS. Competition and cooperation among huddling infant rats.
793 Developmental Psychobiology: The Journal of the International Society for Developmental
794 Psychobiology. 2001;39(2):65-75.
795 56. Wisden W. Sleep and thermoregulation Edward C Harding, Nicholas P Franks and
796 William Wisden. Current Opinion in Physiology. 2020;15:7-13.
797 57. Harding EC, Yu X, Miao A, Andrews N, Ma Y, Ye Z, et al. A neuronal hub binding
798 sleep initiation and body cooling in response to a warm external stimulus. Current Biology.
799 2018;28(14):2263-73. e4.
800 58. Raymann RJ, Swaab DF, Van Someren EJ. Skin deep: enhanced sleep depth by
801 cutaneous temperature manipulation. Brain. 2008;131(2):500-13.
802 59. Gordon C. Thermal physiology of laboratory mice: defining thermoneutrality. Journal
803 of thermal biology. 2012;37(8):654-85.
804 60. Commons KG, Cholanians AB, Babb JA, Ehlinger DG. The rodent forced swim test
805 measures stress-coping strategy, not depression-like behavior. ACS chemical neuroscience.
806 2017;8(5):955-60.
807 61. Iio W, Matsukawa N, Tsukahara T, Kohari D, Toyoda A. Effects of chronic social
808 defeat stress on MAP kinase cascade. Neuroscience letters. 2011;504(3):281-4.
809 62. Hebert M, Evenson A, Lumley L, Meyerhoff J. Effects of acute social defeat on activity
810 in the forced swim test: Parametric studies in DBA/2 mice using a novel measurement device.

811 Aggressive Behavior: Official Journal of the International Society for Research on Aggression.
812 1998;24(4):257-69.
813 63. Iñiguez SD, Riggs LM, Nieto SJ, Dayrit G, Zamora NN, Shawhan KL, et al. Social
814 defeat stress induces a depression-like phenotype in adolescent male c57BL/6 mice. Stress.
815 2014;17(3):247-55.
816 64. Koike H, Ibi D, Mizoguchi H, Nagai T, Nitta A, Takuma K, et al. Behavioral
817 abnormality and pharmacologic response in social isolation-reared mice. Behavioural brain
818 research. 2009;202(1):114-21.
819 65. Berry A, Bellisario V, Capoccia S, Tirassa P, Calza A, Alleva E, et al. Social
820 deprivation stress is a triggering factor for the emergence of anxiety-and depression-like
821 behaviours and leads to reduced brain BDNF levels in C57BL/6J mice.
822 Psychoneuroendocrinology. 2012;37(6):762-72.
823